From Earth to Enlightenment
Materiality, Technology and Cultural Transmission of Terracruda Sculpture Across Buddhist Asia
edited by Mònica López-Prat, Emma Cantisani, Susan S. Bean

A Technical Study of Terracruda Sculpture Fragments from Khara-Khoto

Kaela Nurmi
Fine Arts Museums of San Francisco

Angela Chang
Harvard Art Museums

Katherine Eremin
Harvard Art Museums

Georgina Rayner
Straus Center for Conservation and Technical Studies, Harvard Art Museums

Isabel McWilliams
Iowa State University

Abstract Khara-Khoto was a thriving Buddhist centre of the Tangut-ruled Great Xia empire (1038-1227 CE), producing art that reflected both Himalayan and Chinese traditions. In 1923-24, art historian Langdon Warner removed 250 sculptural fragments, now in the collection of the Harvard Art Museums. Eighteen representative objects were studied to understand their materials and fabrication techniques. Findings included the consistent use of layered clay construction, different internal support systems, modelling, and moulding, a consistent palette of traditional mineral and synthetic pigments, and fragments with ritual deposits.

Keywords Khara-Khoto. Edzina. Tangut. Terracruda. Clay. Polychromy. Micro-CT. Langdon Warner. Ritual deposits.

Summary 1 Introduction. – 1.1 The Site of Khara-Khoto. – 1.2 Khara-Khoto Materials at the Harvard Art Museums. – 1.3 Technical Study Objectives. – 2 Analytical Methods. – 3 Clay and Construction. – 3.1 Clay Composition. – 3.2 Organic Fibres. – 3.3 Forming Techniques. – 3.4 Wooden Armatures and Internal Structures. – 4 Surface Finish and Decoration. – 4.1 Ground Layers and Surface Preparations. – 4.2 Pigments and Polychromy. – 4.3 Repainting. – 4.4 Consolidation and Restoration. – 4.5 Binders. – 5 Discussion. – 6 Conclusion.

Edizioni Ca'Foscari

Marco Polo 6
e-ISSN 2785-5627 | ISSN 2785-5899
ISBN [ebook] 979-12-5742-112-0

Peer review | Open access
Submitted 2026-08-11 | Accepted 2026-09-30 | Published 2026-11-05
© 2026 Nurmi, Chang, Eremin, Rayner, McWilliams | CC BY 4.0
DOI 10.30687/979-12-5742-112-0/005

1 Introduction

1.1 The Site of Khara-Khoto

Khara-Khoto, *Hei Shui Cheng* (黑水城) in Chinese or *Khar Khot* (Хар хот) in Mongolian, was a thriving trade hub and the most northern point of defence for the Tangut-ruled Great Xia dynasty (1038-1227 CE). The Tangut state was distinctly multicultural, maintaining strong diplomatic, religious, and trade ties with Tibet and a complex relationship with Song China. Khara-Khoto flourished as a regional Buddhist centre, producing art reflecting both Himalayan and Chinese traditions. In 1227, the Tangut state, including Khara-Khoto, was toppled during Genghis Khan's final campaign. Marco Polo visited Khara-Khoto in the late 13th century when it was under Mongol rule, referring to it as Edzina in his travel documents. The city was abandoned in the 14th century during the Ming dynasty.

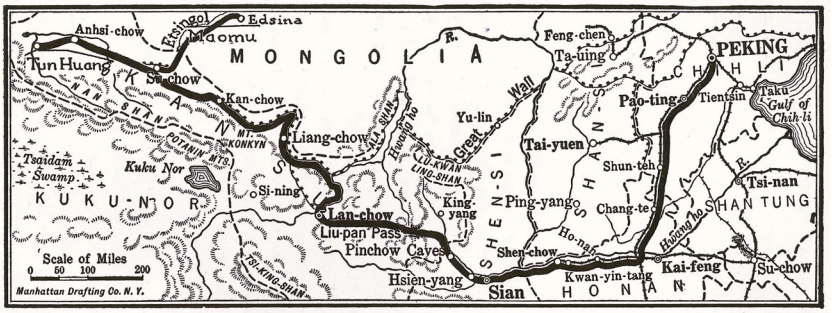


Figure 1 Map of Warner's 1923-24 expedition route with Khara-Khoto labelled as 'Edsina' (Warner 1926, 12)

The walled city of Khara-Khoto formed an irregular rectangle (440 x 370 m) with gateways on the east and west walls. At its peak, the interior had many buildings, stupas, and temples. As an oasis situated near the Ejin River (also referred to as Edzingol or Etsingol), the city used a network of canals for irrigation. The Tangut economy was based on agriculture and animal husbandry, with skilled ironworking and ceramic production (Kychanov 1993, 54). While direct evidence is limited, Khara-Khoto likely participated in these regional practices. The densely populated city prospered, with merchant caravans passing through between China and lands to its West.

Located in modern-day Inner Mongolia, Khara-Khoto was the destination of three expeditions in the early twentieth century. In 1908, Russian explorer Pyotr Kuzmich Kozlov, funded by the Imperial treasury, disturbed structures and stupas and removed objects without systematic documentation. These portable paintings and objects are now housed at the State Hermitage Museum in St. Petersburg. In 1914, archaeologist Sir Marc Aurel Stein, funded by the government of British India, sifted through the remains left by Kozlov's team and collected a range of materials, now divided amongst the National Museum, New Delhi, and the British Museum, London (Stein 1928, 447).

Archaeologist and art historian Langdon Warner led the First Fogg Expedition to China (1923-24), which was organised by the Fogg Museum of Harvard University and launched as a bold effort to enhance the Fogg Museum's collection of Asian art (Bewer 2010, 114). Closely following the footsteps of Kozlov and Stein and eager to join their ranks, Warner was intent on bringing back what remnants he could from the site. Warner and a team of local workers spent ten days excavating at Khara-Khoto, collecting approximately 250 objects, primarily air-dried clay figural sculptures, mould-made plaques, architectural elements, and small votive objects. Warner likely retrieved many objects in the rubble along the base of the city wall, caused by previous disturbances to the site. He named his route from Peking to Khara-Khoto (which he called Edsina, following Marco Polo) and to the cave site of Dunhuang (Tun Huang), 'The Long Old Road in China' **[fig. 1]** – the same title used for his published account of the journey (Warner 1926). During the expedition, he photographed the remains of Khara-Khoto and other sites **[fig. 2]**.

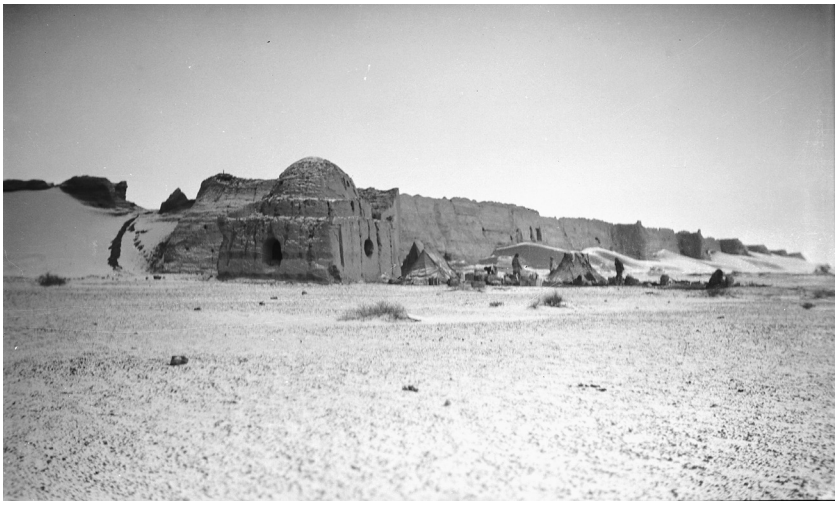


Figure 2 Warner, L. (1923-24). Khara Koto, view of ruins nestled against cliffs from afar, barren land in foreground. Langdon Warner Collection, Harvard Fine Arts Library, Special Collections. Cambridge, Massachusetts, USA, [Public domain]

Given that the Xia empire was one of a thriving community of Tanguts, Chinese, Uyghurs, Khitans, and Tibetans, its artistic and visual culture was distinctly multicultural. Tangut Buddhist art, as is also found in excavated pagodas, shows the close co-existence of Chinese and Himalayan styles (Linrothe 1995). The fragile nature of the *terracruda* sculptures that Warner brought back to Harvard has long signalled the likelihood of local manufacture over Tibetan import to art historians, speaking to the movements of artists, monks, and portable objects along the routes connecting Khara-Khoto and the Western Himalayas. Furthermore, studies have shown how royal Xia patronage of Esoteric Buddhism strengthened the Tanguts' relationship with Tibet and participation within a network beyond the Xia borders (Meinert 2020). The harmonious co-existence of Chinese and Himalayan styles and the local activity of multicultural artistic devotion are present in the Khara-Khoto materials at the Harvard Art Museums.

1.2 Khara-Khoto Materials at the Harvard Art Museums

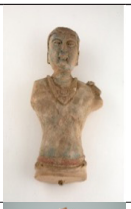
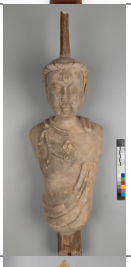
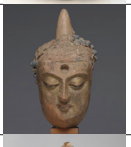
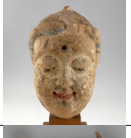
The objects brought to Harvard from the 1923-24 First Fogg Expedition illustrate the range of air-dried clay object types from the site, including figural sculptures, architectural elements, plaques, and votive objects. While these objects share close affinities with Tibetan sculpture, they uniquely attest to local production in the Khara-Khoto region, suggesting that the artistic connections between Tangut and Himalayan societies influenced local Tangut Buddhist practice, devotional image making, and architectural adornment (Klimburg-Salter 1982, 119).

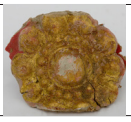
1.3 Technical Study Objectives

The collection of Khara-Khoto materials at the Harvard Art Museums has remained unpublished since entering the museum in 1924. This paper reports on the technical investigation of eighteen representative fragmentary air-dried clay objects with polychrome decoration, detailed in Table 1. Based on size, construction methods, and comparisons with other sites on the Silk Roads, the figural fragments and roundels were components of larger architectural settings, though their original contexts remain unknown. Similarly, the small plaques and votives were deposited within stupas or left as offerings within these settings. Thus, all of the objects may be described as monumental terracruda sculpture: raw earth-based objects made *in situ* and linked to their surroundings, such as an architectural framework or monument (López-Prat et al. 2024). Differences in the degree of finish for some objects suggest that they were intended for different display contexts. For example, the back of Torso_12 is roughly finished, with incised striations in multiple directions across the clay surface. This contrasts with the smooth, even front surface. The rough back was likely positioned against a wall or other architectural element.

Table 1 Objects included in technical study

Accession Number	Image	Title	Dimensions	Term in Paper
1924.65.2		*Headless Seated Figure*	18.4 × 14 × 10.5 cm	Torso_2
1924.65.6		*Headless Seated Figure*	15.2 × 18.4 × 12.1 cm	Torso_6
1924.65.7		*Sculpture Fragment: Torso and Arms of a Figure*	19 × 17.5 × 6.5 cm	Torso_7

Accession Number	Image	Title	Dimensions	Term in Paper
1924.65.12		*Head and Torso of a Bodhisattva*	31 × 15 × 8 cm	Torso_12
1924.65.18		*Headless Standing Figure*	69.5 × 23 × 20 cm	Torso_18
1924.65.23		*Head and Torso possibly of an Eleven-Headed Avalokiteshvara*	58.5 × 18 cm	Torso_23
1924.65.24		*Head and Torso of a Seated Figure*	28 × 16.5 × 10.5 cm	Torso_24
1924.65.11		*Head of a Buddha*	22 × 12 × 13 cm	Head_11
1924.65.20		*Head of a Buddha*	16 × 12 × 13 cm	Head_20
1924.65.5.D		*Figure Fragment*	3 × 5 × 13 cm	Arm_5D
1924.65.27		*Lotus Architectural Roundel*	16 × 16 × 7 cm	Roundel_27
1924.65.34.M		*Small Architectural Stupa*	7 × 8.5 × 8.5 cm	Tsatsa_34M

Accession Number	Image	Title	Dimensions	Term in Paper
1924.65.36.F		*Stippled Votive Stupa*	7.5 × 7.5 × 7.5 cm	Tsatsa_36F
1924.65.32.F		*Plaque in the form of a Head*	4 × 2.7 × 1.3 cm	Plaque_32F
1924.65.32.K		*Plaque in the form of a Head*	4.8 × 2.3 × 1.3 cm	Plaque_32K
1924.65.40.G		*Fragment of a Plaque with colour pigments*	0.8 × 2.8 × 3 cm	Plaque_40G
1924.65.40.K		*Fragment of a Plaque with colour pigments*	2.5 × 3.8 × 1 cm	Plaque_40K
1924.65.40.Q		*Fragment of a Plaque with colour pigments*	3 × 1.6 × 2.5 cm	Plaque_40Q

2 Analytical Methods

Visual examination complemented a multi-analytical approach to investigate object construction and material composition. X-radiography and micro-computed tomography (micro-CT) were used to study construction methods. Polychromed surfaces were first analysed with in-situ X-ray fluorescence (XRF) to determine likely pigments based on the elemental composition. For a more complete understanding of the materials and their relationships, micro-samples were taken from areas of loss or damage. Excised samples were analysed by Fourier-transform infrared spectroscopy (FTIR) and Raman spectroscopy to characterise pigments and applied organic materials. Where possible, samples were mounted and polished to provide cross-sections for optical microscopy (OM) and scanning electron microscopy with energy dispersive X-ray spectroscopy (SEM-EDS) to examine stratigraphy and identify specific pigments and preparatory layers. Samples of clay were removed from the underside or damaged areas of three objects to investigate the clay substrate using FTIR, SEM-EDS and X-ray diffraction (XRD). Fibres embedded within the clay matrix were examined using polarised light microscopy (PLM). Finally, selected wooden elements were sampled for accelerator mass spectrometry (AMS) radiocarbon dating at the University of Georgia. Further analytical details can be found in Chang et al. (2025).

3 Clay and Construction

The figural fragments are made from clay mixtures, applied in layers over different styles of armatures or cast in moulds. The clay composition, as characterised by analysis, is described below, followed by details of the armatures, forming techniques, and ritual deposits observed with X-radiography imaging.

3.1 Clay Composition

Preliminary XRD of clay samples from three objects identified quartz, calcite, and gypsum, and showed weak signals from sheet silicates such as illite and/or kaolinite. FTIR analysis confirmed the presence of strong -OH absorption bands from hydrated sheet silicates. This suggests the clay was not fired at or above 400 ^{0}C, although rehydration of sheet silicates cannot be ruled out.

SEM-EDS analysis of cross-sections with clay identified silicates such as quartz, feldspars, mica and clay minerals (likely illite-group), carbonates such as calcite and (sparse) dolomite, and iron oxides. Talc, another sheet silicate, is present between the pigment and clay, likely as a white ground layer. The relative proportions of clays (with high aluminium and potassium) and non-silicates (calcite and/or gypsum) differ significantly between samples. Full distinction of the different minerals and their proportions, particularly sheet silicates, would require larger samples for quantitative XRD. Overall, the clay mixture is broadly similar across the study group, suggesting a consistent approach to clay preparation and to the formulation of surface layers.

3.2 Organic Fibres

Organic fibres are distributed throughout the clay matrix, providing further evidence for the use of air-dried clay rather than fired ceramic. The quantity and visibility of organic fibres within the clay vary considerably, ranging from sparse, fine fibres to abundant, coarse bundles. Sampling was limited to objects with accessible fibres at the surface, and it was not possible to obtain fibres from any figural objects. Fibres were sampled from Roundel_27 and Plaque_40Q, both of which are likely mould-made from a single clay body rather than constructed from multiple applied layers.

The clay body of these objects contains both fine and coarse plant materials distributed through the matrix, visible at the surface of the reverse impression. PLM identified a bast fibre in the fine material and straw in the coarse material. It is likely that the figural sculptures contain similar plant materials incorporated into the clay matrix to deliberately modify the working and drying properties of the air-dried clay.

3.3 Forming Techniques

All sculptural objects in the study group exhibit layered construction with variations in execution, as revealed through X-radiography and micro-CT scanning. In virtual micro-CT cross-sections, voids visible between clay layers indicate successive additions of the material.



Figure 3 Torso_2, micro-CT 'slice' views across (a) the torso and arms and (b) crossed legs, with (c) slice locations indicated with red lines. Three pieces of wood (dark rectangles) support the legs.
© President and Fellows of Harvard College



Figure 4 Head_20, micro-CT profile (a) and X-radiograph frontal (b) views show layers of successively fine clay packed around a wood armature. Embedded behind each eye is a round, flattened radio-dense object that appears bright white in the image. A third, similar object, not visible in the X-radiograph, was observed between the eyes through micro-CT. Clay was packed over these objects, which are not visible on the surface

In smaller figural sculptures, uniformly textured clay layers were added to simple internal structures. For example, in Torso_2, clay was built up around a bundle of fibres (see 3.4) in pieces and layers, with the arms added last **[fig. 3]**.

In contrast, larger sculpture fragments exhibit more varied internal structures. The core clay is coarser, containing abundant inclusions (likely organic). For Head_20, the clay is built around a solid wooden support. Clay packed around the wood is granular with irregular air pockets and variably sized inclusions; layers of clay are finer and more uniform towards the surface **[fig. 4]**. While larger figural sculptures were modelled directly and developed with applied elements, smaller forms and some details were mould-made.

The face on Torso_24 and two of the three faces on Torso_23 show evidence they were pressed into an open mould: the overall thickness is uniform, thin layers and underlying voids in the clay follow the arc of the face, and the backs of the forms are smooth from pressing the clay. The resulting 'masks' are integrated with the core structure, showing irregular gaps where they are attached to a fine homogeneous clay **[fig. 5]**. By contrast, the large face on Torso_23 is thinner and more variable in thickness, likely modelled *in situ* onto the coarse underlayer. The multiple faces suggest that this sculpture was originally an image of the eleven-faced Avalokiteśvara *bodhisattva*.

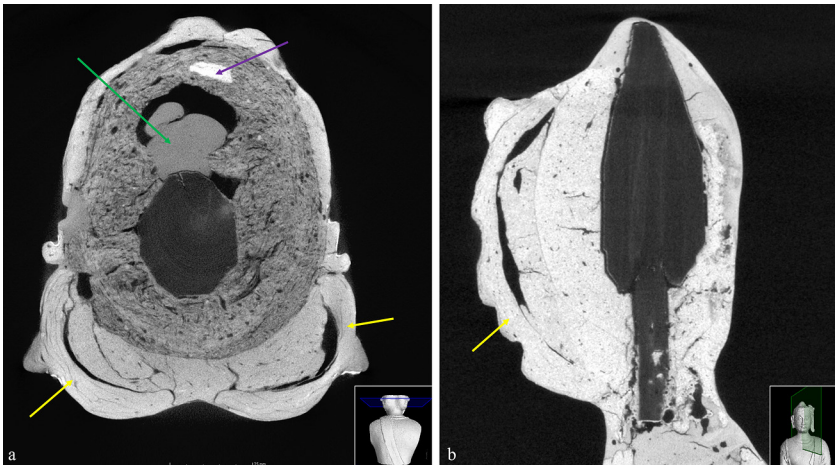


Figure 5 Micro-CT views of (a) Torso_23, horizontal section across head (location indicated by small image at lower right corner), showing mould-made face 'masks' (yellow arrows) with underlying voids, modern plaster (green arrows) and a ferrous ritual deposit (purple arrow); (b) Torso_24, profile, showing mould-made face 'mask' with underlying void

The observed distinction between fine surface clay and coarser interior layers likely reflects different structural and aesthetic purposes: the coarse mixture with fibres is stronger and bulks out the form, and the finer mixture can be modelled or moulded with sharp details to make a smooth surface for painting. Small, mould-made objects such as plaques and *tsatsas* do not require the supporting coarse layer.

3.4 Wooden Armatures and Internal Structures

Though varied, all figural sculpture fragments contain internal wooden armatures. A summary of non-clay materials identified within the sculptural fragments is presented in Table 2.

Radiocarbon dating was carried out on some wood samples to verify their 12th-century attribution. Results from three figural pieces, Torsos 2, 7, and 23, show distinct chronological differences between the three samples, summarized in Table 3. While radiocarbon dating indicates when wood ceases to exchange carbon with the atmosphere, rather than when the sculpture was made, the results suggest that Torso_7 is earlier, and Torso_2 is later than the 12th-century. These results point to a more complicated chronology for the Khara-Khoto objects and warrant further investigation.

Table 2 Non-clay materials observed

Object	Wood	Twine/lashing material	Metal hardware	Other organic material
Torso_2	Yes	No	No	Yes
Torso_6	Yes	No	No	No
Torso_7	Yes	Yes	No	No
Torso_12	Yes	No	No	No
Torso_18	Yes	No	Yes	No
Torso_23	Yes	No	Yes	No
Torso_24	Yes	No	No	No
Arm_5D	Yes	Yes	No	No
Head_11	No	No	No	Yes
Head_20	Yes	No	No	No

Table 3 Radiocarbon dating of select wood samples

Object	Wood sampled	Calibrated date (95%)[1]
Torso_2	Exposed piece in seated base	1217-70 CE
Torso_7	Exposed armature in torso	993-1035 CE
Torso_23	Armature extending from bottom of object	1043-1213 CE

1 Radiocarbon dates were calibrated with IntCal120.14c and reported at 95% (2s) certainty.

3.4.1 Comparison of Armature Systems

Internal armatures were categorised into three main types: vertical post(s), horizontal crossbars, and wood incorporated into arms, summarized in Table 4.

Table 4 Armature types inside figural sculptures

Object	Vertical posts(s)	Horizontal crossbar	Wood in arms	Notes
Torso_2	No	No	No	Bundle of organic fibres forms the core. Wood pieces in the legs
Torso_6	Yes	No	No	Two vertical posts, clay slabs
Torso_7	Yes	Yes	Yes	Bundle of vertical sticks; horizontal stick at shoulders
Torso_12	Yes	No	No	Additional wood piece in head
Torso_18	Yes	Yes	Yes	Crossbar at hips
Torso_23	Yes	Yes	No	Crossbar at shoulders
Torso_24	Yes	No	No	Conical shape in head (separate from vertical wood in torso)
Arm_5D	No	No	Yes	Twine wrapped around length of wood
Head_11	No	No	No	Bundle of organic strands forms the core
Head_20	Yes	No	No	Irregularly shaped wood, all one piece

Although similarly scaled, the seated figures Torso_2 and Torso_6 feature different internal structures. The core of Torso_2 is formed from a vertical bundle of organic fibres cinched together at the top and at the waist with a horizontal tie, probably made of the same type of fibre. Below the waist, a bundle has been lost, though fibre impressions in the clay remain **[figs 3, 6a]**. Head_11 has a similar structure **[figs 10a-b]**. Within the crossed legs, three unconnected pieces of wood provide internal structural support. In contrast, Torso_6 is built around two vertical wooden supports arranged together, though not visibly bound. Micro-CT revealed vertical clay slabs flanking the supports and other horizontal slabs in the lap **[fig. 6]**. Formed separately and added, the slabs appear to serve as rigid support and bulk in thick sections of the body. The slabs' grain and composition are visually similar to the surrounding clay. No slab elements were observed in the other objects.

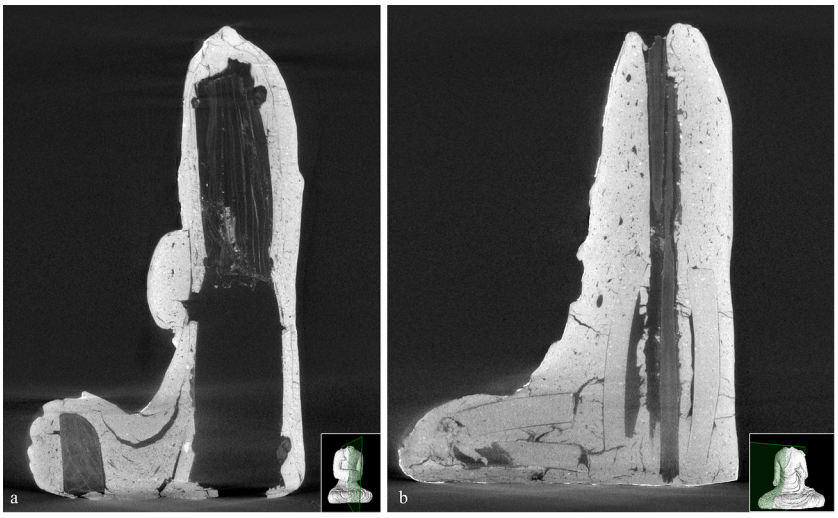


Figure 6 Micro-CT images comparing core structures of (a) Torso_2 and (b) Torso_6. Slice locations are indicated by small reference images, lower left corners. © President and Fellows of Harvard College

3.4.2 Binding Systems and Metal Fasteners

A twine-like organic binding material was observed in multiple objects. The armature for Torso_7, consisting of three vertical supports, is bound together at the waist, while Arm_5D has twine wrapped along the length of the wooden armature and lashes around another armature element inside the elbow **[figs 7-8]**. The wrapped twine would also have provided texture to help the clay bond to this armature.

Metal hardware was also used to secure internal wooden elements. The largest sculptures, Torso_18 and Torso_23, incorporate ferrous metal fasteners (tested with a magnet), with irregular faceted and tapered shanks to connect internal wooden elements and reinforce cross-shaped armatures **[fig. 9]**.

Torso_18 has a central vertical wooden support with a horizontal crossbar at hip level secured by multiple nails. Two supports for the lower body are fastened to the crossbar with nails. A sizable nail at each shoulder appears to connect supports for the arms to the central vertical element through a layer of clay. A modern metal rod has been inserted into the figure through the base.

Micro-CT of Torso_23 shows a broad, horizontal crossmember fastened to the central vertical post at the chest. The crossmember is joined using a lap joint and secured with a ferrous metal nail. Nails at both ends of the crossmember correspond with areas of loss and plaster repairs, suggesting they may have originally secured additional structural components or arms.

Micro-CT of Torso_23 also reveals that the visible wooden column is continuous, extending through the torso and principal head, serving as the structure for the smaller faces of the eleven-faced Avalokiteśvara *bodhisattva* (see Linrothe 1996, 38).

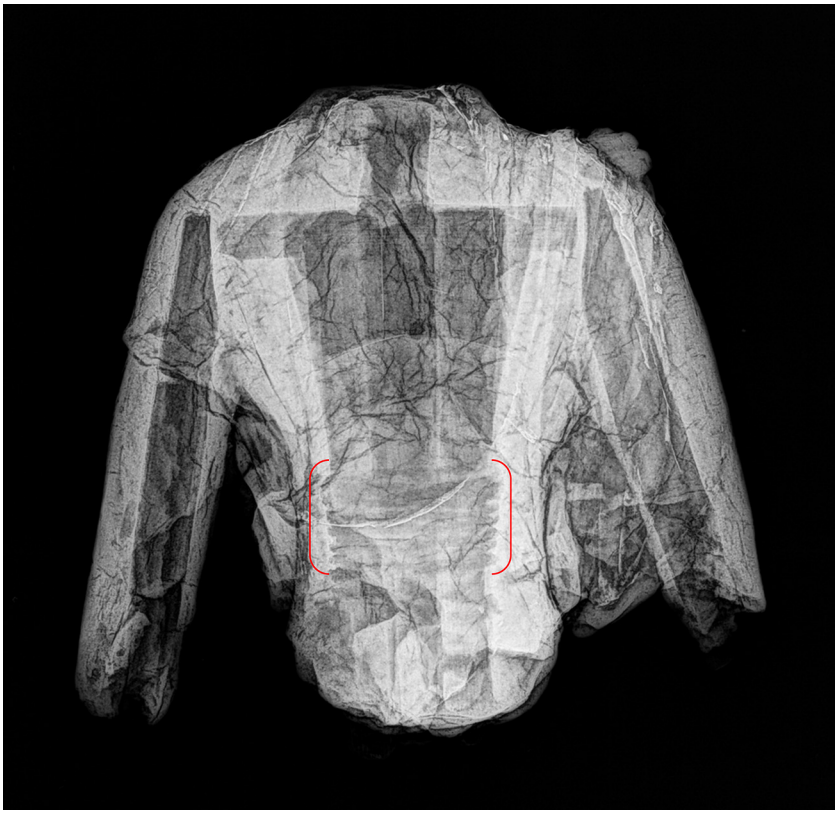


Figure 7 Torso_7, X-radiograph showing binding (within red brackets) around the armature components at the waist.
© President and Fellows of Harvard College



Figure 8 (a) Arm_5D, a loss on the back reveals a twine-wrapped armature; (b) Arm_5D, X-radiograph shows wrapping along the wooden support and binding another element at the elbow. © President and Fellows of Harvard College



Figure 9 (a) X-radiograph of Torso_23; (b) top half Torso_18. © President and Fellows of Harvard College

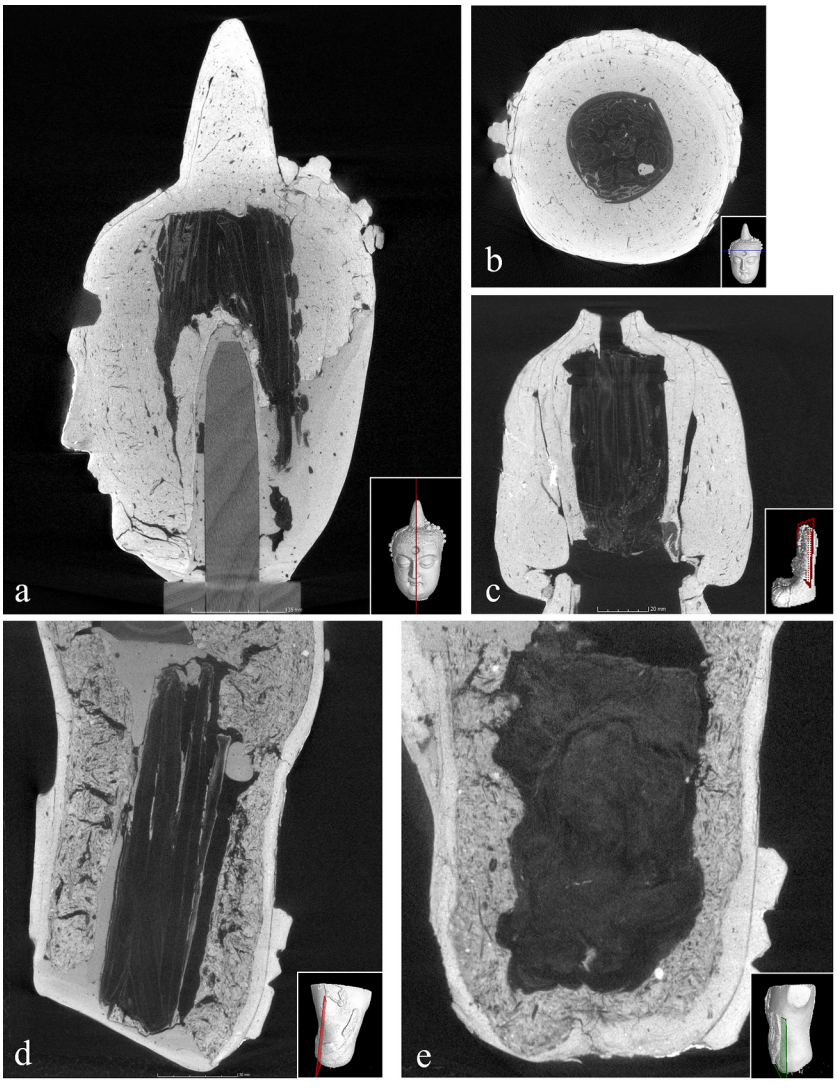


Figure 10 Micro-CT images: (a) Head_11, core comprised of organic fibres; (b) Head_11, horizontal slice showing crescent-shaped cross sections of fibres; (c) Torso_2 fibres arranged around small clay chunks in the upper back; (d) Torso_23 fibres in the lower torso, proper right side; (e) Torso_23, slice across front, lower torso containing a mass of finer, fibrous material, possibly wool. © President and Fellows of Harvard College

3.4.3 Unidentified Materials

Micro-CT imaging revealed numerous instances of materials deposited within the clay body during fabrication. The long, folded fibrous strands forming the core in Torso_2 and Head_11 are also found in Torso_23, packed within the proper right side of the abdomen [fig. 10d]. Each strand has a crescent-shaped cross-section up to 1 cm wide [figs 3a, 10a]. Their plain, hollow morphology resembles that of reeds. In Head_11, Torso_2, and Torso_23, there is modern plaster adjacent to the strands, indicating they

were exposed during a repair. The closely packed clay and imprints from the strands indicate they are original.

Torso_23 contains a second cavity in the lower abdomen positioned in a flat, wide space in front of the central timber **[fig. 10e]**. This encloses a distinct mass of an organic material with fine, clumped fibres, possibly wool.

The small stupa-shaped *tsatsas* provide a related devotional context in which incorporated organic materials could be examined directly. Fibrous organic materials are incorporated into some of the *tsatsas* as evidenced by broken examples exposing bundles of dark brown, wiry, hair-like material within the air-dried clay. Microscopic examination of a sample from Tsatsa_34 found that the morphology was consistent with hair. Further analysis and microscopy could help characterise the hair and other organic materials identified in the figural *terracruda* sculptures, although access for sampling is limited. In addition to the organic materials discovered in Torso_23, three small deposits, presumed to be stone, metal, or another radio-dense material, were discovered: one embedded in the clay behind the eyes **[fig. 5]**, one on the proper left side of the lower torso, and one in the belly within the wool-like mass. Head_20 contains three similar elements embedded in the head, one behind each eye, and a third between the eyes **[fig. 4]**.

4 Surface Finish and Decoration

The air-dried clay fragments exhibit complex and visually rich polychrome decoration with similar pigments in all object types. To identify the pigments, all colours were analysed initially with in-situ XRF to determine the main inorganic elements present. This was followed by sampling in areas of loss or flaking. In some instances, only in-situ XRF was possible due to later-applied surface consolidation. Unmounted samples were analysed by FTIR and Raman spectroscopy. Mounted samples were analysed with SEM-EDS, revealing multiple layers in some samples. The materials and layers identified with SEM-EDS analysis are summarized in Table 5.

Table 5 Summary of analysis of pigments on objects studied, with gold and silver content of gilding in weight percentage (wt%). Abbreviations used in table: PL – proper left; PR – proper right; NX – geometry did not allow XRF analysis; NS – not sampled; NA – sample not available (whole sample mounted); NP – no peaks; and NM – sample not mounted for SEM (too small)

Colour	Object	Location	XRF	FTIR	Raman	SEM (pigment layer)
Red	Torso_2	neck (dark red)	Fe, (Pb)	Calcite, kaolin, quartz	Hematite, quartz	Fe, Pb, Cl
		PL sleeve	Fe, (Pb)	Calcite, kaolin, quartz	Hematite, quartz	Fe, Pb, Cl
		PR sleeve	Hg, (Pb, Fe)	Kaolin, quartz	Vermilion	NM
	Torso_6	PR arm	Hg, Pb, (Cu, Fe)	Calcite, gypsum?, kaolin, quartz	Vermilion	Hg, S, (Pb, Cl)
	Arm_5D	wrist	Fe	Kaolin, quartz	Hematite, quartz	NM
	Torso_7	PL sleeve	Hg, Pb, (Ca)	Calcite, kaolin	Vermilion, red lead, calcite	NM
	Torso_12	belt	Hg, (Ca, As, Pb)	Calcite, kaolin	Vermilion	Hg, S, Ca
	Torso_18	robe (dark red)	Hg, (Pb)	Calcite, kaolin, talc	Vermilion	Hg, S
		robe (pink)	Hg, (Pb)	Calcite, talc	Vermilion	Hg, S, Pb
		robe (maroon)	Fe, (Pb)	Kaolin, quartz	Hematite, magnetite or hausmanite	Fe, Si, Al
	Torso_23	face	Hg	Gypsum?, talc?	Vermilion	Hg, S, (Ca, Mg, Si, Al)
		sash (orange-red)	Hg, (Fe)	Calcite, gypsum?, talc	Vermilion	Hg, S, (Ca, Mg, Si, Al)
	Torso_24	robe	Hg, Pb	Calcite, kaolin	Vermilion, red lead, calcite	Hg, S, Pb
	Head_11	lips	NX	Calcite, gypsum, quartz	Vermilion	NM
	Head_20	lips	Hg, (Pb)	Calcite	Vermilion	NM
	Head_20	Chin (pink)	Pb, (Hg)	NS	NS	NS
	Roundel_27	Top (pink under gold)	Au, (Fe, Ag)	Calcite, gypsum?, talc	Hematite	NM
	Plaque_32F	PR eye	Hg, Pb	Lead white	Vermilion, lead white	Hg, S, Pb, Cl
	Plaque_40Q	edge	Hg	Mica, quartz	Vermilion	NM
	Tsatsa_36F	surface (orange-red)	Fe	Gypsum, kaolin, quartz	Hematite, quartz	Fe, Si, Al
Yellow	Torso_2	drapery	As, (Cu, Fe)	Calcite	Orpiment	NM
	Plaque_40G	top	As, S	Gypsum?, kaolin?, talc?	Orpiment	NM

Colour	Object	Location	XRF	FTIR	Raman	SEM (pigment layer)
Green	Torso_2	legs	As, Ca, (Pb)	Calcite, kaolin quartz,	Carbon black indigo, orpiment	NM
	Torso_6	drapery (with white)	Cu, Cl, As, Pb, Sn, (Ca)	Atacamite, calcite, kaolin	Atacamite, orpiment vermilion	Cu, Cl, Sn; over lower layers with As, S & Hg, S
	Torso_7	PR robes	Cu, As, (Ca)	Atacamite, brochantite	Atacamite, orpiment	As, S; over Cu, Cl, S, Si, Pb, Sn
	Torso_18	PR sleeve	Cu Cl, Sn, Pb, As	Atacamite	Vermilion	Cu, Cl, S, Pb, Sn
		PL sleeve	NX	Atacamite	Atacamite	Cu, Cl, S, Pb, Sn
	Torso_24	PR robe	Cu, Cl, Pb, Sn	Atacamite	calcite	NM
	Head_11	mustache	NX	Atacamite	NP	NM
	Head_20	chin	Cu, (Pb, Cl, Sn)	Atacamite, lead white	Atacamite, azurite	NM
Blue	Torso_7	back	Fe, Ca, As	Calcite, indigo	Indigo, orpiment	As, S, Si Al; over C-rich blue layer
		PR arm	Cu	NA	NA	Cu, Ca, Pb
	Torso_12	face; skin	Cu, (Ca)	Azurite, calcite, gypsum, kaolin,	Azurite	NM
	Torso_18	PL skirt	Cu, (As)	Azurite, calcite, talc	Azurite, indigo	Cu, Ca, Mg, Si
		ribbon	Cu, Fe, (Ca, Pb)	Azurite, talc	Azurite, hematite	NM
		back	Cu	Azurite, kaolin, quartz	Azurite	Cu, Fe, Si, Al
	Torso_23	hair	Cu, (Ca, Pb)	Azurite, kaolin	Azurite	Cu, Fe, Si, Al
	Torso_24	PL arm	Cu	Azurite, mica	Azurite	NM
	Head_11	PL hair curl	Ca, (Fe, Pb)	Calcite, indigo, quartz	Indigo, calcite	NM
		PR hair curl	Cu, (Ca)	Calcite, kaolin, quartz	Azurite, carbon black, indigo	NM
	Head_20	hair	Cu	Azurite, kaolin, quartz	Azurite, vermilion, quartz	NM
	Arm_5D	hand	Cu, Ca	Azurite, calcite, kaolin	Azurite, calcite	Cu

Colour	Object	Location	XRF	FTIR	Raman	SEM (pigment layer)
White	Torso_7	shirt	Pb, (As, Ca)	Lead white, calcite talc	Lead white, hematite,orpiment, vermilion	Pb, Hg, S
		below other colours	Ca	NS	NS	NS
	Torso_12	body	Ca	NS	NS	NS
	Torso_18	PR sleeve	Ca	Calcite, gypsum?, talc	NP	NM
		decoration on drapery	Pb	NS	NS	NS
	Torso_23	face	Fe, (Ca, As, Pb)	Calcite, gypsum, talc	Dolomite, gypsum	Pb, Cl, Hg, S
	Torso_24	below other colours	Ca	NS	NS	NS
		chest	Ca	Calcite, gypsum, kaolin, quartz	Calcite	NM
		PL robe	Ca, (Pb)	Calcite, gypsum, kaolin, quartz	Calcite	NM
	Head_11	eye	Pb	NS	NS	NS
	Head_20	PR skin (with red)	(Pb, Hg)	Calcite, gypsum, kaolin, quartz	Calcite, gypsum, vermilion	Cu, Cl, Pb, Sn, Ca (green); over Pb, Ca, Hg, S, Cl (white with red)
	Arm_5D	below blue	Ca	NS	NS	NS
Black	Torso_12	PR eye	Ca, (Pb)	Calcite, huntite, kaolin	Carbon black	NM
		PR hair	Ca, (Fe)	Calcite, gypsum	Carbon black	NM
		hair	Ca, (Fe)	Calcite, gypsum, kaolin	Carbon black	NM
	Plaque_32K	hair	Like clay	Huntite, kaolin, quartz	Carbon black	Carbon-rich, Ca, S
Gold	Torso_6	PR arm	As, Pb, Hg, Au (Fe)	NA	NA	Au 94, Ag 6, <1 µm; over As, S; over Hg, S
	Torso_18	robe	Au, As	Gypsum?, talc	NP	Au 94, Ag 8, 2 µm; over As, S
	Head_11	PL eye (over pink)	Au, Hg, (Ag)	NA	NA	Au 94, Ag 6, 5 µm, multiple compressed layers; over Hg, S
	Roundel_27	top (over pink)	Au, (Ag)	Calcite, huntite, gypsum?, talc	Hematite	Au 92, Ag 8, <1 µm; over Mg, Si, Al, Fe
	Plaque_40K	top (over pink)	Au, (Ag)	Calcite, gypsum, talc	NP	Au 94, Ag 6, <1 µm; over Mg, Si, Al, Fe,
	Plaque_40Q	outside petal	Au, Pb	Gypsum, talc?	NP	Au 88, Ag 12, 3 µm; over Hg, Pb. Cl

4.1 Ground Layers and Surface Preparations

Coloured pigments were applied over white ground layers of talc (magnesium- and silicon-rich layers in SEM-EDX), kaolin, and/or calcite which overlie the clay. In some samples, gypsum occurs within the ground layer and/or upper part of the clay substrate. Thin layers of gypsum may be due to alteration of an original alum sealant on the clay surface, as proposed at Dunhuang (Wong, Agnew 2013). However, thicker layers of gypsum were likely applied deliberately. Lead white and lead chloride were also present, likely as white surface layers rather than a preparatory or priming ground.

4.2 Pigments and Polychromy

4.2.1 Red

The dominant red pigments are red ochre (containing hematite) and mercuric sulfide, cinnabar or vermilion. The fine particle size suggests use of synthetic vermilion rather than natural cinnabar. Red ochre and vermilion were often used separately in different areas of a single figure. Red lead was relatively rare and only used in combination with vermilion.

4.2.2 Yellow

Orpiment was the only yellow pigment identified, used alone and combined with indigo for green.

4.2.3 Green

Atacamite was the main green pigment, with occasional mixtures of orpiment and indigo. Malachite was not identified in any sample, although azurite occasionally occurs with atacamite. SEM-EDS showed that tin- and lead-rich inclusions occur within some atacamite particles, and copper sulfate is mixed with atacamite in Torso_18. In Torso_7, brochantite is intergrown with copper-containing silicates and mixed with atacamite. Yong (2012) found that synthetic production of copper chloride pigments began to dominate the green pigments used in China from the 10th century. The morphology of the particles was used to determine the nature of the copper chloride pigment: angular particles were attributed to natural copper chloride, rounded to spherical particles to synthetic copper chloride (Yong 2012). The angular morphology of the atacamite particles in these samples is hence more consistent with use of natural atacamite. Similarly, the intergrowths and morphology of atacamite, brochantite, and azurite suggest a natural source – a mixed deposit of atacamite with other minerals.

4.2.4 Blue

Azurite and indigo were the only blue pigments identified. These were normally used separately: azurite for lighter, brighter blues, and indigo for

darker blues. Mixtures of azurite and indigo occur in only two instances. A dark blue hair curl from Head_11 contains azurite, indigo, and carbon black, whilst the adjacent lighter blue hair curl contains only indigo. Similarly, azurite and indigo are present in the blue skirt of Torso_18, whilst other blue areas of the figure only contain azurite. These variations may indicate the selection of different mixtures to achieve a specific blue.

4.2.5 White

White pigments include kaolin, talc, calcite, and gypsum, used for ground layers and white details, and occasional lead white and lead chloride in paint layers and details. Lead white is notably more opaque than the other white materials. A pink tint was created on some figures using layers of lead white containing vermilion with different particle sizes. In many samples, thin layers of lead chloride are present alone, within layers of lead white, or as scattered particles mixed with other pigments. Lead chloride may have been deliberately used in mixtures, perhaps as a less opaque white than lead white. Colour blending with lead oxychloride and other pigments was noted at the Tiantishan grottos (Zhou, Zhang, Cheng 1997).

4.2.6 Black

Carbon black was used as the black pigment.

4.2.7 Gold

Gilding is present on six objects. Most samples show a single layer of extremely thin gold foil (less than 3 microns) with some overlapping and crumpled edges. However, multiple layers of compressed, crumpled gold foil are present in the sample from Head_11. Most foil is high purity gold with only 6-8 wt% silver, with one example containing 12 wt% silver. The gold foil was often applied over coloured layers, with simple layering of gold over talc and red ochre in Roundel_27 and Plaque_40K, and over vermilion in Plaque_40Q. More complex layering occurs on the figures: gold was applied over orpiment and vermilion in Torso_6, and gold was used over orpiment and red ochre in Torso_18.

4.3 Repainting

Cross-sections from four objects, Torso_6, Torso_7, Head_20, and Plaque_32F, contain multiple coloured layers. The composition of these layers is given in Table 5. The pigments in all layers are the same as those used elsewhere, and the colour change is often minimal, suggesting historic repainting, documented at cave sites including Dunhuang (Shui et al. 2022) and Yungang (Piqué 1997).

4.4 Consolidation and Restoration

Cellulose nitrate, available in the early 20th century, was detected with FTIR in most figural sculptures, apart from Torso_6 and Arm_5D. Many surfaces are covered in fine sand-like particulates, with heavy concentrations in the interstices of the decoration. The particulate is trapped in place by the consolidation layer, suggesting hasty application during the excavation or shortly after the sculpture arrived at Harvard. Unfortunately, there are no extant treatment records documenting this modern consolidation.

Torso_18 has an applied layer of poly(vinyl acetate), available from ca. 1930, and cellulose nitrate on the surface, both identified with FTIR. Some areas of this figure also had evidence of restoration in the form of chromium green pigments, available from the late 19th or 20th century, and Prussian blue, available from the 18th century. However, there are no records of when restoration occurred.

4.5 Binders

Protein was detected with FTIR in paint samples from two figures (Torso_7 and 18), Roundel_27, and Plaques_32K, 40G, 40Q. However, all samples from the figures contain cellulose nitrate, and the roundel and plaques have a glossy surface despite the lack of detectable cellulose nitrate. This evidence of previous treatment prompts caution in the interpretation of results. Although there is some evidence for use of a protein-based binder, further investigation is required to distinguish between its presence as an original binder or later restoration material.

5 Discussion

The figural sculptures examined follow a sequence of manufacture consistent with the common elements of monumental *terracruda* sculpture as described by López-Prat et al. (2024) and aligned with earlier practices in greater Gandhara and India, as described by Tarzi (1986) and Varma (1987), respectively, as well as at Dunhuang (Chang et al. 2026). The figural sculptures studied provide insights into technical consistencies and variability of air-dried sculptural forms at Khara-Khoto.

The variability in armature designs demonstrates object-specific construction practices using wood as a primary structural support. For larger figures, a central wooden post was necessary for structural integrity. In Torso_23, the substantial column extending through and beyond the figure may have supported the visages of an eleven-faced bodhisattva. If so, it would be the only sculpture of its form to survive in the Tangut corpus; painted examples remain at the State Hermitage Museum and on the wall of Yulin Cave 3. For smaller, compact figures, such as Torso_6, wooden armatures may not have been structurally necessary, though their use has reinforced their enduring forms. The bundle of organic fibres serving as a core in Torso_2 was packed directly with clay, though the fibres have shrunken, leaving their original impressions in the clay. Torso_7, similar in scale, has extended arms, which do require internal support. Wooden

elements were secured together with twine or metal nails, particularly in larger sculptures.

Clay was added to internal frameworks in successive layers, progressing from coarser structural clay to finer exterior modelling layers. Within several objects, the discovery of similar materials placed within the clay bodies during the manufacture is particularly significant: these objects (perhaps metal or stone) and organic materials may be ritual deposits or symbolic organs, akin to those found in Buddhist sculptures of different media across cultures. The recurring strands, used as a structural core in Torso_2 and Head_11, but deposited in a discrete, non-structural bundle in Torso_23, warrant further investigation. Although material identification requiring samples is limited due to the deposits' inaccessibility, identification with micro-CT at higher resolution may be possible.

Applied details, modelled or cast in moulds, were attached to the sculpture. The use of moulds aligns with the evidence of extensive use of moulds for clay-based sculptures across sites on the Northern Silk Road (Schmidt 2025, 152-3) and described by Tarzi (1986) in sites at Hadda.

The surfaces were finished with a fine layer of clay, often covered with whitish ground containing mixtures of talc, calcite, and/or gypsum. Polychrome decoration was applied over the white ground using a palette of mineral and manufactured pigments, including red ochre, vermilion, azurite, indigo, atacamite, orpiment, talc, calcite, gypsum, lead white, and lead chloride. This assemblage is consistent with pigments used from the late Tang onwards, particularly the lack of malachite and lazurite, scarcity of red lead compared to vermilion and hematite, and use of lead white.[2] Thin layers of gilding were added in the final stages of surface decoration. A protein-based binding medium, likely animal glue, may have been employed as a binder in the paint layers.

Notably, there was no detection of smalt on any clay sculpture. This contrasts with an early identification of smalt from a fragment of a wall painting attributed to Khara-Khoto and given to Gettens by Langdon Warner in 1925 (Gettens, Stout [1942] 1966, 159; Mühlethaler, Thissen 1969, 48-9, 57; 1993, 114, 128). This fragment was reportedly taken to the Smithsonian by Gettens but has yet to be located. Gettens' identification has frequently been referenced as the earliest occurrence of smalt in Eurasia. However, recent examination of the three wall paintings, several unidentified clay fragments with remaining pigment, and the clay objects presented here found only azurite and indigo with no smalt detected.

6 Conclusion

This technical investigation provides the first comprehensive study of materials and construction technologies of air-dried clay objects from Khara-Khoto. The results demonstrate that sculptural production at the site was based on layered clay construction, diverse internal support systems, hybrid moulding and hand-modelling techniques, and a consistent palette of mineral and synthetic pigments. Several fragments included more than one

2 Piqué 1997; Wainwright et al. 1997; Li 2002; Wong, Agnew 2013; Liu et al. 2016; Shui et al. 2022.

ritual deposit. These techniques align with broader traditions of Buddhist monumental *terracruda* sculpture while exhibiting their own characteristics.

Having remained largely unexamined for a century, the Harvard Art Museums' holdings of Khara-Khoto fragments provided an exceptional opportunity to investigate the materials and technologies of Tangut Xia clay sculpture. Visual examination and analytical evidence confirmed that these objects are air-dried clay, resolving inconsistencies in museum records (which had variously categorised them as unfired clay, ceramic, and sun-dried clay) and establishing more accurate and consistent terminology for future documentation. Additionally, micro-CT imaging proved to be an effective, non-invasive tool for investigating internal structure, morphology, distribution, and assembly of components.

This study provides an important technical foundation for future scholarship and conservation of the fragments, as well as related traditions of *terracruda* sculpture across the Silk Roads. The rich findings from this small group of objects have prompted interest in the identification and study of the internal ritual deposits, as well as an expanded technical study of remaining fragments at the Harvard Art Museums to further illuminate artistic practices at Khara-Khoto.

Acknowledgements

The authors thank Sarah Laursen, Alan J. Dworsky curator of Chinese Art for her support of this project, Richard Newman and Timothy Cavanaugh for their help with SEM at the Museum of Fine Arts Boston and at Harvard University Center for Nanoscale Systems (CNS) respectively, Celia S. Chari for analysing clay samples by FTIR and XRD at CNS, and H. Greg Lin who performed micro-CT at CNS. CNS is a member of the National Nanotechnology Coordinated Infrastructure Network (NNCI), which is supported by the National Science Foundation under NSF award no. ECCS-2025158.

Bibliography

Bewer, F. (2010). *A Laboratory for Art: Harvard's Fogg Museum and the Emergence of Conservation in America, 1900-1950*. Cambridge: Harvard Art Museums.

Chang, A.; Eremin, K.; Degryse, P.; Rayner, G.; Laursen, S. (2025). "Technical Findings on Objects from Afghanistan at the Harvard Art Museums". Vanleene, A.; Marguier, A.; Brice, V. (eds), *Artists and Artisans: Representations of an Era of Religious Images*. Strasbourg: Université de Strasbourg, 71-105. https://www.calameo.com/books/007213666e456314ace06

Chang, A.; Eremin, K.; Rayner, G.; McWilliams, I. (2026). "A Technical Study of *Kneeling Attendant Bodhisattva* from the Mogao Caves, Dunhuang". López-Prat, M.; Cantisani, E.; Bean, S.S. (eds), *From Earth to Enlightenment: Materiality, Technology and Cultural Transmission in Buddhist Monumental Terracruda Sculpture*. Venice: Edizioni Ca' Foscari, 73-90. https://doi.org/10.30687/979-12-5742-112-0/004.

Gettens, R.; Stout, G. [1942] (1966). *Painting Materials: A Short Encyclopaedia*. New York: Dover Publications.

Klimburg-Salter, D. (1982). *The Silk Route and the Diamond Path: Esoteric Buddhist Art on the Trans-Himalayan Trade Route*s. Los Angeles: UCLA Art Council.

Kychanov, E.I. (1993). "The State of Great Xia (982-1227 A.D.)". Piotrovsky, M. (ed.), *Lost Empire of the Silk Road: Buddhist Art from Khara Khoto (X-XIII Century)/The State Hermitage Museum*. Milano: Electa, 49-58.

Li, Z. (2002). Pigment analysis on Tang Dynasty murals at the Mogao Grottoes [敦煌莫高窟唐代绘画颜料分析研究]. *Dunhuang Research* [敦煌研究], 2002(4), 11-18, 110.

Liu, L.; Shen, W.; Zhang, B.; Ma, Q. (2016). "Microchemical Study of Pigments and Binders in Polychrome Relics from Maiji Mountain Grottoes in Northwestern China". *Microscopy and Microanalysis*, 22, 845-56. https://doi.org/10.1017/S1431927616011302.

Linrothe, R. (1995). "Peripheral Visions: On Recent Finds of Tangut Buddhist Art". *Monumenta serica*, 43, 235-62.

Linrothe, R. (1996). "New Delhi and New England: Old Collections of Tangut Art". *Orientations*, 27(3), 32-41.

López-Prat, M.; Pecci, A.; Lancelotti, C.; Miriello, D. (2024). "Shaping the Sacred along the Silk Roads: The Millenary Artistic Tradition of Making 'Monumental Terracruda Sculptures'". *Journal of Archaeological Science: Reports*, 54, 104454. https://doi.org/10.1016/j.jasrep.2024.104454.

Meinert, C. (2020). "Creation of Tantric Sacred Spaces in Eastern Central Asia". Meinert, C.; Sørensen, H. (eds), *Buddhism in Central Asia I: Patronage, Legitimation, Sacred Space, and Pilgrimage*. Leiden; Boston: Brill, 244-72.

Mühlethaler, B.; Thissen, J. (1969). "Smalt". *Studies in Conservation*, 14(2), 47-61.

Mühlethaler, B.; Thissen, J. (1993). "Smalt". Roy, A. (ed.), *Artists' Pigments: A Handbook of Their History and Characteristics*, vol. 2. Washington: National Gallery of Art, 113-30.

Piqué, F. (1997). "Scientific Examination of the Sculptural Polychromy of Cave 6 at Yungang". Agnew, N. (ed.), *Conservation of Ancient Sites on the Silk Road = Conference Proceedings* (Dunhuang, 3-8 October 1993). Los Angeles: Getty Conservation Institute, 348-61.

Schmidt, B. (2025). "Technical Analysis on Buddhist Clay-Based Sculptures from the Northern Silk Road. A Preliminary Comparison with Greater Gandhāra". Vanleene, A.; Marguier, A.; Brice, V. (eds), *Artists and Artisans: Representations of an Era of Religious Images*. Strasbourg: Université de Strasbourg, 147-65. https://www.calameo.com/books/007213666e456314ace06.

Shui, B.; Yu, Z.; Cui, Q.; Wang, Z.; Yin, Z.; Sun, M.; Su, B. (2022). "Blue pigments in Cave 256, Mogao Grottoes: a systematic analysis of murals and statues in Five dynasties, Song Dynasty and Qing Dynasty". *Heritage Science*, 10(1), 89. https://doi.org/10.1186/s40494-022-00722-5.

Stein, A. (1928). *Innermost Asia: Detailed Report of Explorations in Central Asia, Kan-Su and Eastern Irān*. Oxford: Clarendon Press.

Tarzi, Z. (1986). "La technique du modelage en argile en Asie Centrale et au Nord-Ouest de l'Inde sous les Kouchans: La continuité malgré les ruptures". *Ktèma: Civilisations de l'Orient, de la Grèce et de Rome antiques*, 11(1), 57-94. https://doi.org/10.3406/ktema.1986.2635.

Varma, K.M. (1987). *Technique of Gandhāran and Indo-Afghan Stucco Images: Including Images of Gypsum Compound*. Santiniketan, India: Proddu.

Wainwright, I.; Moffat, E.; Sirois, J.; Young, G. (1997). "Analysis of Wall Painting Fragments from the Mogao and Bingling Grottoes". Agnew, N. (ed.), *Conservation of Ancient Sites on the Silk Road = Conference Proceedings* (Dunhuang, 3-8 October 1993). Los Angeles: Getty Conservation Institute, 334-40.

Warner, L. (1926). *The Long Old Road in China*. Garden City: Doubleday, Page & Company.

Wong, L.; Agnew, N. (eds) (2013). *Conservation of Cave 85 at the Mogao Grottoes*. Los Angeles: Getty Conservation Institute. https://www.getty.edu/publications-reports/item/241X04.

Yong, L. (2012). "Copper Trihydroxychlorides as Pigments in China". *Studies in Conservation*, 57(2), 106-11. https://doi.org/10.1179/2047058411Y.0000000008.

Zhou, G.; Zhang, J.; Cheng, H. (1997). "Pigment Analysis of Polychrome Statuary and Wall Paintings of the Tiantishan Grottoes". Agnew, N. (ed.), *Conservation of Ancient Sites on the Silk Road: Proceedings of an International Conference on the Conservation of Grotto Sites*. Los Angeles: Getty Conservation Institute, 362-8.

Zhou, Z.; Shen, L.; Zhang, H. (2021). "The Wall Painting Techniques and Materials of Kizil Grottoes". Aoki, S.; Taniguchi, Y.; Rickerby, S.; Mori, M.; Kijima, T.; Su, B.; Kirino, F. (eds), *Conservation and Painting Techniques of Wall Paintings on the Ancient Silk Road*. Singapore: Springer, 231-51. Cultural Heritage Science. https://doi.org/10.1007/978-981-33-4161-6_13.